Kinematic Optimisation of the Gantry-Tau Parallel Kinematic Manipulator with respect to its Workspace

Ilya Tyapin & Geir Hovland
ITEE, The University of Queensland
Brisbane, Australia QLD 4072
Email: {ilya,hovland}@itee.uq.edu.au

Torgny Brogårdh
ABB Robotics
SE-721 68 Västerås, Sweden
Email: torgny.brogardh@se.abb.com

Abstract

The Gantry-Tau is a recently developed parallel kinematic manipulator (PKM). Since the actuators are stationary it possesses the following characteristics: high speed, high acceleration, small moving mass and high static and dynamic accuracy. Since all link forces in the structure are axial, high stiffness can also be achieved.

One of the main advantages of the Gantry-Tau machine is a large workspace area in comparison with traditional parallel machines. However, parameters of the machine, such as link lengths and dimension of support frames, can be difficult to design manually. In this paper we present a method to optimise such parameters to achieve the largest possible workspace. The problem is solved by using a non-linear optimisation routine and imposing the parameterisation on the midpoints of three spheres generated by the parallel links that intersect at the tool center point (TCP).

1 Introduction

The Tau family of parallel kinematic manipulators (PKM) was invented by ABB Robotics, see [Brogårdh, 2002]. The Gantry-Tau was designed to overcome the workspace limitations while retaining many advantages of PKMs such as low moving mass, high stiffness and no link twisting or bending moments. For a given Cartesian position of the robot each arm has two optimal solutions for the inverse kinematics, referred to as the left- and right-handed configurations. While operating the Gantry-Tau in both left- and right-handed configurations, the workspace will be significantly larger in comparison with a serial Gantry-type robot with the same footprint.

In this paper we consider the triangular-link variant of the 3-degree-of-freedom (DOF) Gantry-Tau structure, which was first presented in [Brogårdh, 2005]. Triangular mounted links give several advantages: they enable a reconfiguration of the robot, a larger reach is obtained in the extremes of the workspace. When using parallel links, the orientation of the manipulated platform will be constant, which increases the risk of collisions of the arms with the manipulated platform in the extremes of the workspace area. At the platform end of the links, 3-DOF universal joints are used. At the actuator end of the links, 2-DOF joints are used.

In [Johannesson, 2004] an optimisation method for the 3-DOF Gantry-Tau with no triangular links was presented. Two geometrical parameters of the machine, Q_1 and Q_2, were optimised to maximise the cross-sectional workspace area. Q_1 is the overall height and Q_2 is the overall width of the machine. These two parameters were chosen because they determine the required installation space of the robot. Our paper is an extension of the work in [Johannesson, 2004]. The new contributions of this paper are: the optimisation is made for the Gantry-Tau with triangular mounted links and the optimisation is made of the whole workspace volume and not just the cross-sectional workspace area. When optimising the volume, the fixed lengths of the linear actuators must be taken into account.

In the past many researchers focused on the calculation of the workspace area of PKMs. In order to calculate the workspace one can employ discretisation methods, geometrical methods or analytical methods. For the discretisation method a grid of nodes with position and orientation is defined. Then the kinematics is calculated for each node and it is straightforward to verify whether the kinematics can be solved and to check if joint limits are reached or link interference occurs [Dashy, 2002]. The discretisation algorithm is simple to implement but has some serious drawbacks. It is expensive in computational time and results are limited to the nodes of the grid.

Analytical workspace area methods investigate the properties of the kinematic transmission [Goldenberg,

1985], [Angeles, 1985]. Most approaches are based on the inverse kinematics because it can typically be solved in closed form and it is easer to distinguish between multiple solutions. Whereas discretisation methods are based on the full inverse kinematics, the analytic approaches usually only require parts of the inverse kinematics. Even so, analytical methods can be expensive in computational time.

Using geometrical methods the constant orientation workspace can be calculated as an intersection of simple geometrical objects [Merlet, 1995], for example spheres. The midpoints of the spheres are found from the pivot points for e.g. PUS (prismatic joint, universal joint, spherical joint) and UPS (legs form a cylinder and a sphere). Constraints on the joints and on the articulated coordinates can be introduced through further restrictions on the geometrical entities and the intersection of these objects can be done with the techniques that are known from computer aided design (CAD). Examples of such constraints are floors, ceilings and prismatic joint locations to avoid collisions with the links.

In this paper a geometrical method for the Gantry-Tau that uses parameterisation of the midpoints of the three spheres that intersect at the TCP [Johannesson, 2004] is used. Section 2 briefly describes the kinematics and the configuration of the triangular-link version of the Gantry-Tau. The geometrical workspace calculations are described in Section 3. Section 4 describes the non-linear optimisation method to find the solution of the sphere midpoints which results in the largest possible workspace volume. Finally, the optimisation results are described in Section 5.

2 Kinematic Description

The kinematics of the basic Gantry-Tau structure has been described earlier in [Johannesson, 2004]. In this paper we consider the triangular-link version of the Gantry-Tau structure, which is illustrated in Fig. 1, 3 and 4.

As for the basic Gantry-Tau structure, the position of one end of each of the 3 parallel arms (lengths L_1, L_2 and L_3) is controlled by a linear actuator with actuation variables q_1, q_2 and q_3. The actuators in Fig. 1 are aligned in the direction of the global X coordinate. The arm connected to actuator q_1 consists of one single link. The arm connected to actuator q_2 consists of two parallel links. The arm connected to actuator q_3 consists of three links, where two links are mounted in a triangular configuration.

Fig. 2 shows for arm 3 the linear actuator variable q_3, the triangular mounted links and the single link in parallel with the plane formed by the triangular links. Because of the construction of this arm, the passive joint angles are related as follows: $q_{1c} = q_{1d} = q_{1e}$ and $q_{2c} = q_{2d} = q_{2e}$. For example, q_{1c} is a rotation about the y-direction of the link connected to platform point **C** and q_{2c} is a rotation about the new x-direction of the same link. These angles are equal for a nominal robot model. Small errors in the link lengths will cause the link angles to differ. The subscripts a to f refer to the platform connection points **A** to **F** defined in Fig. 3. The spheres in Fig. 2 labelled m_{3c}, m_{3d}, m_{3e}, refer to the joints on the TCP platform labelled **C**, **D** and **E** in Fig. 3.

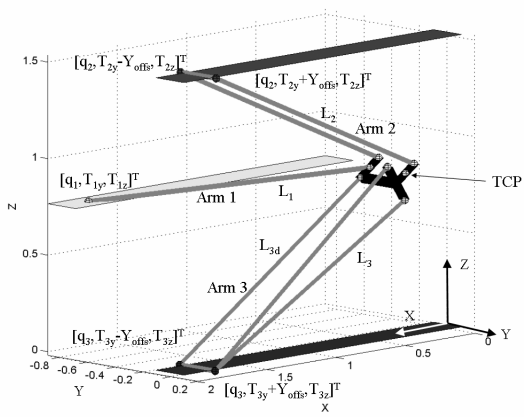

Figure 1: The triangular arm version of the Gantry-Tau.

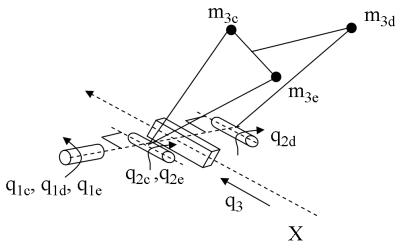

Figure 2: Coordinate frames of arm 3.

The difference in this version of the Gantry-Tau compared to the basic version analysed in [Johannesson, 2004] is that two of the links in the three-link arm are mounted in a triangular constellation instead of in parallel. Note that the link which is in parallel with the triangular link pair has a length of L_{3d}, which is slightly smaller than L_3.

Fig. 3 shows the manipulated platform. The points **A**, **B**, **C**, **D**, **E** and **F** are the link connection points. The arm with one single link connects the actuator q_1 with platform point F. The arm with two links connects actuator q_2 with the platform points **A** and **B**. The arm with three links connects actuator q_3 with the platform points **C**, **D** and **E**. The triangular pair is connected to points **C** and **E**.

The lengths L_4, L_5, L_6, L_7 and L_8 are constant platform parameters. In Section 3 a workspace cross-sectional area function is developed. This function uses

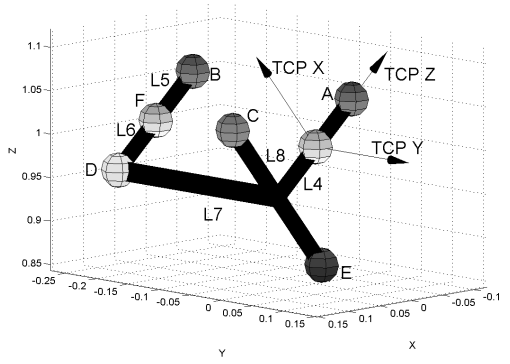

Figure 3: Manipulated platform.

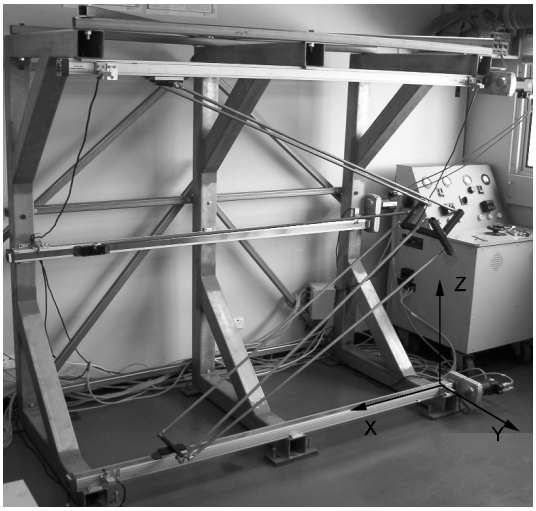

Figure 4: The Gantry-Tau prototype at the University of Queensland.

the arm lengths L_1, L_2 and L_{3d} plus the platform lengths L_4 to L_8.

3 Workspace Area and Volume Functions

The workspace in the X-direction is limited by the length of the linear actuators. Care must also be taken to avoid collisions between the arms, platforms and actuators. Fig. 5 shows three circles, one for each arm. The centres of the circles are located at the actuator positions. The radii of the circles equal the arm lengths plus the distance from the end of the arm to the TCP. For example, the radius of circle 3 equals $L_{3d} + L_4$. The TCP can only reach points inside all of the circles. Fig. 5 also contains three solid lines in the YZ-plane. Because of potential collisions, the TCP is not allowed to move outside these lines which indicate the support framework positions. The valid TCP positions are illustrated in grey in Fig. 5. In the following text, an analytic, closed-form solution for the grey area in Fig. 5 is presented. For the application of the method the parameters for the prototype in Fig. 4 will be used. Here the arm lengths plus the distances from the ends of the arms to the TCP are $L_1^{''} = L_2^{''}$, $L_{3d}^{''}$ and equal to the radii of the circles. The lower and upper actuator limits are at X_L and X_U. The cross-sectional area in Fig. 5 is valid when $x \in [x_3; x_4]$, where x_3 and x_4 will be defined in Section 5.

In the following equations the arm lengths with superscript $''$ are equal to the radii of the circles, for example, $L_{3d}^{''} = L_{3d} + L_4$.

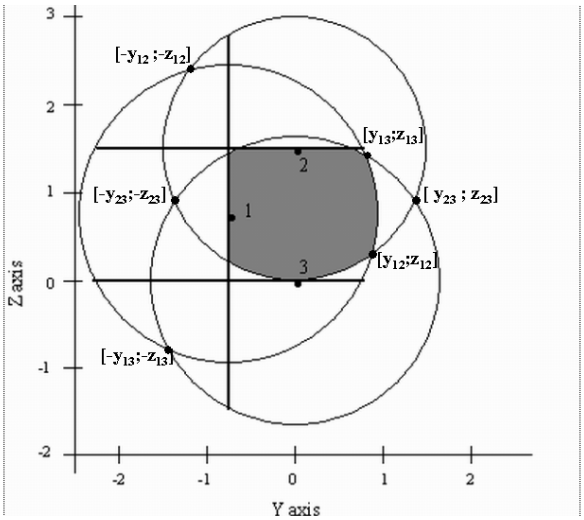

Figure 5: The constant workspace area of the Gantry-Tau machine in the YZ-plane.

The fixed y- and z-coordinates of the track positions T_{iy} and T_{iz} where $i = 1, 2, 3$ are given below. Note that the optimisation parameters Q_1 and Q_2 are introduced here, where the track positions T_{2z}, T_{1y} and T_{1z} depend on Q_1 and Q_2. The track positions are defined in Fig. 1.

The goal of the optimisation is to find the values of Q_1 and Q_2 that result in the largest possible workspace volume.

$$T_{3y} = 0 \quad (1)$$

$$T_{3z} = 0 \quad (2)$$

$$T_{2y} = T_{3y} \quad (3)$$

$$T_{2z} = T_{3z} + Q_2 \quad (4)$$

$$T_{1y} = T_{3y} - Q_1 \quad (5)$$

$$T_{1z} = \frac{(T_{2z} + T_{3z})}{2} \quad (6)$$

The midpoints of the spheres in the YZ-plane are then given by: sphere 1: $[T_{1y}, T_{1z}]$, sphere 2: $[T_{2y}, T_{2z}]$ and

sphere 3: $[T_{3y}, T_{3z}]$. Given the midpoints, the functions that describe the circles are given below.

$$(T_{1y} - y)^2 + (T_{1z} - z)^2 = L_1^{'2} \quad (7)$$

$$(T_{2y} - y)^2 + (T_{2z} - z)^2 = L_2^{'2} \quad (8)$$

$$(T_{3y} - y)^2 + (T_{3z} - z)^2 = L_{3d}^{'2} \quad (9)$$

Note the notation with the single superscripts $'$ which will be introduced later in this section.

The y-coordinates of the cross points between circle number 2 and 3 are illustrated in Fig. 5 and are given below.

$$y_{23} = \pm\frac{\sqrt{-(L_2'^2 - L_{3d}'^2 - T_{2z}^2)^2 + 4L_{3d}'^2 T_{2z}^2}}{4T_{2z}^2} \quad (10)$$

If y_{23} is not a real number, then there is no common cross-point between circles 2 and 3. In this case, the cross-sectional area will be zero. The early detection of a zero workspace is an advantage of a geometric workspace area approach compared to a solution based on the inverse kinematics. If y_{23} is real, then the cross-points between circles 1 and 3, 1 and 2 and 2 and 3 can be calculated.

The y-coordinates of the cross-points between circles 1 and 3 are given below, where k_1 is a help variable.

$$\begin{aligned} k_1 &= (L_1^{'2} - L_{3d}^{'2} - T_{1z}^2 - T_{1y}^2)T_{1y} \\ y_{13} &= \frac{-k_1 \pm \sqrt{k_1^2 - 4(T_{1y}^2 + T_{1z}^2)(\frac{k_1^2}{4T_{1y}^2} - L_{3d}'^2 T_{1z}^2)}}{2(T_{1y}^2 + T_{1z}^2)} \end{aligned} \quad (11)$$

The y-coordinates of the cross-points between circles 1 and 2, y_{12}, are shown below, where k_2 to k_6 are help variables.

$$\begin{aligned} k_2 &= T_{1y}^2 + L_2^{'2} - T_{2z}^2 + T_{1z}^2 - L_1^{'2} \\ k_3 &= 4k_2(T_{1z} - T_{2z}) + 8T_{1y}^2 T_{2z} \\ k_4 &= -4T_{1y}^2 - 4(T_{1z} - T_{2z})^2 \\ k_5 &= -4T_{1y}^2 T_{2z}^2 - k_2^2 + 4T_{1y}^2 L_2^{'2} \\ k_6 &= \sqrt{k_3^2 - 4k_4 k_5} \\ z_{12} &= \frac{-k_3 \pm k_6}{2k_4} \quad (12) \\ y_{12} &= \pm\sqrt{L_2'^2 - (T_{2z} - z_{12})^2} \quad (13) \end{aligned}$$

The workspace is divided into 4 areas A_1, A_2, A_3 and A_4 as illustrated in Fig. 6, 7 and 8. For example, A_2 in Fig. 6 will be a rectangle for small values of Q_2. At bigger values of Q_2 the upper limit will be partly circular and partly constant. The total cross-sectional area A_T is given by

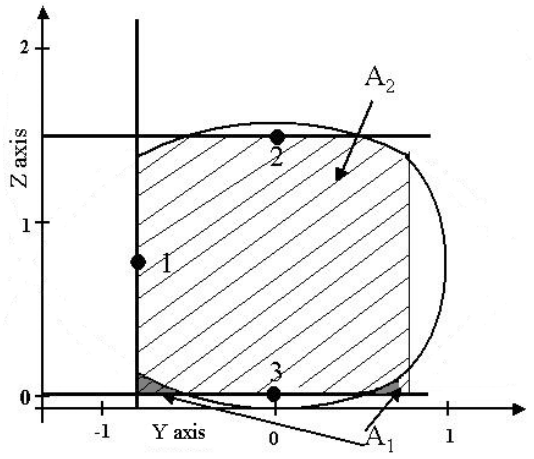

Figure 6: Illustration of workspace area 1 and 2.

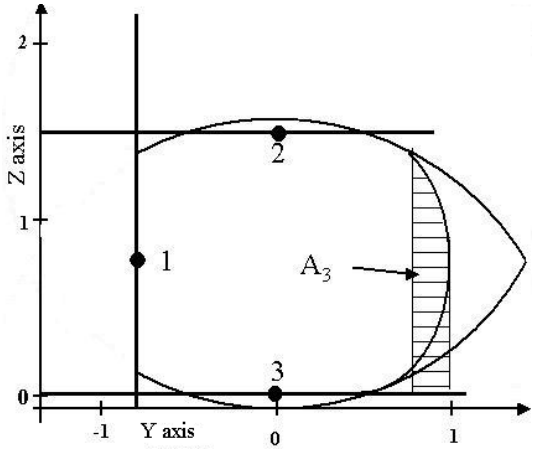

Figure 7: Illustration of workspace area 3.

$$A_T = A_2 + A_3 - A_1 - A_4 \quad (14)$$

Simpson's rule is used to approximate the individual area functions. For example, A_1 is given by

$$\begin{aligned} A_1 \simeq \frac{h}{3}[&f_1(y_0) + 4f_1(y_1) + 2f_1(y_2) + 4f_1(y_3) + ... \\ &+2f_1(y_{n-2}) + 4f_1(y_{n-1}) + f_1(y_n)] \end{aligned} \quad (15)$$

Where h is a step of the iteration and equals $\frac{(y_0+y_n)}{n}$. n, an even number, represents the number of divisions on the Y-axis.

The function $f_1(y)$ above is given by

$$f_1(y) = T_{2z} - \sqrt{T_{2z}^2 - y^2 - T_{2z}^2 + L_2'^2} \quad (16)$$

The function $f_1(y)$ is found from equations (7)-(9) by expressing the z-coordinate as a function of the y-coordinate.

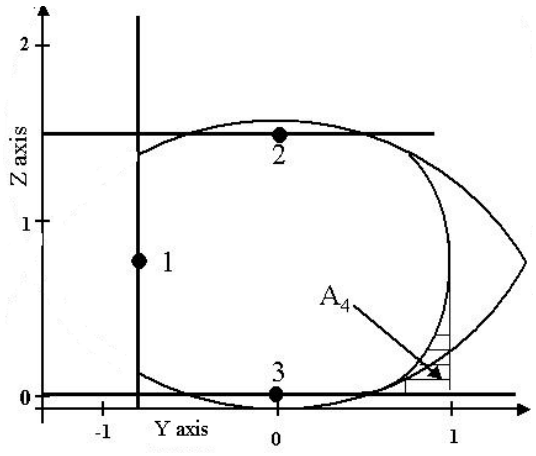

Figure 8: Illustration of workspace area 4.

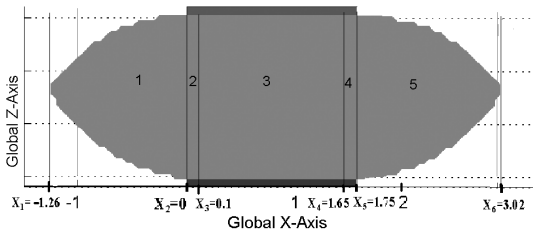

Figure 9: The workspace area of Gantry-Tau machine in the XZ-plane when it is reconfigured to work in both positive and negative x-direction.

The other areas A_2 to A_4 are found in a similar way to A_1, using the functions $f_2(y)$ to $f_4(y)$ given below.

$$f_2(y) = \sqrt{L_{3d}^{'2} - y^2} \quad (17)$$

$$f_3(y) = T_{1z} + \sqrt{T_{1z}^2 - ((T_{1y} - y)^2 + T_{1z}^2 - L_1^{'2})} \quad (18)$$

$$f_4(y) = T_{1z} + \sqrt{T_{1z}^2 - ((T_{1y} - y)^2 + T_{1z}^2 - L_1^{'2})} \quad (19)$$

The next step is to calculate the workspace volume as a function of the cross-sectional areas. If A_T is not a real number, then the TCP cannot reach that point with the given x-coordinate. If A_T is real, then the volume function can be calculated as

$$V = \sum_{x=x_1}^{x=x_6} A_T(x)\delta \quad (20)$$

where δ is a step of the summation and $A_T(x)$ is a workspace area for the given x-coordinate.

Firstly, upper and lower bounds x_1 and x_6 for TCP on the X-axis must be found, and following this, additional bounds $x_2, \cdots, x_5$, that depend on the kinematics must be determined. These additional bounds are actuator limits $x_2 = X_L$ and $x_5 = X_U$, plus offsets x_3 and x_4 given by the offset Y_{offs} illustrated in Fig. 1. Following this, new radii for the three circles have to be found, one for each robot arm. The new radii depend on the given x position. Finally, the cross-sectional workspace area can be calculated. Some different workspace areas for the given x positions are presented in Fig. 10

The 6 bounds $x_1, x_2, x_3, x_4, x_5, x_6$ define 5 sections on the global X-axis. The sections are $[x_1; x_2], [x_2; x_3], [x_3; x_4], [x_4; x_5], [x_5; x_6]$. These 5 sections are numbered in Fig. 9. The TCP can only reach points with x-coordinates between x_1 and x_6. Between these limits, the cross-sectional area varies as illustrated in Fig. 9 and Fig. 10.

The radii for the three circles in Fig. 5 depend on the x-coordinate. For the section $x \in [x_1; x_2]$ the radii are defined as follows.

$$L_1^{'} = \sqrt{L_1^{''2} - (x - x_2)^2} \quad (21)$$

$$L_2^{'} = \sqrt{L_2^{''2} - (x - x_3)^2} \quad (22)$$

$$L_{3d}^{'} = \sqrt{L_{3d}^{''2} - (x - x_3)^2} \quad (23)$$

The single superscript $'$ as mentioned earlier denotes the section-dependent circle radii. The double superscript $''$ denote the nominal circle radii.

The circle radii for the second section $x \in [x_2; x_3]$ are defined as:

$$L_1^{'} = L_1^{''} \quad (24)$$

$$L_2^{'} = \sqrt{L_2^{''2} - (x - x_3)^2} \quad (25)$$

$$L_{3d}^{'} = \sqrt{L_{3d}^{''2} - (x - x_3)^2} \quad (26)$$

In the third section $x \in [x_3; x_4]$ the radii equal the nominal values, ie.

$$L_1^{'} = L_1^{''} \quad (27)$$

$$L_2^{'} = L_2^{''} \quad (28)$$

$$L_{3d}^{'} = L_{3d}^{''} \quad (29)$$

In the fourth section $x \in [x_4; x_5]$ the radii equal

$$L_1^{'} = L_1^{''} \quad (30)$$

$$L_2^{'} = \sqrt{L_2^{''2} - (x - x_4)^2} \quad (31)$$

$$L_{3d}^{'} = \sqrt{L_{3d}^{''2} - (x - x_4)^2} \quad (32)$$

Finally, the radii in the fifth section when $x \in [x_5; x_6]$ equal

$$L_1^{'} = \sqrt{L_1^{'2} - (x - x_5)^2} \quad (33)$$

$$L_2^{'} = \sqrt{L_2^{'2} - (x - x_4)^2} \quad (34)$$

$$L_{3d}^{'} = \sqrt{L_{3d}^{'2} - (x - x_4)^2} \quad (35)$$

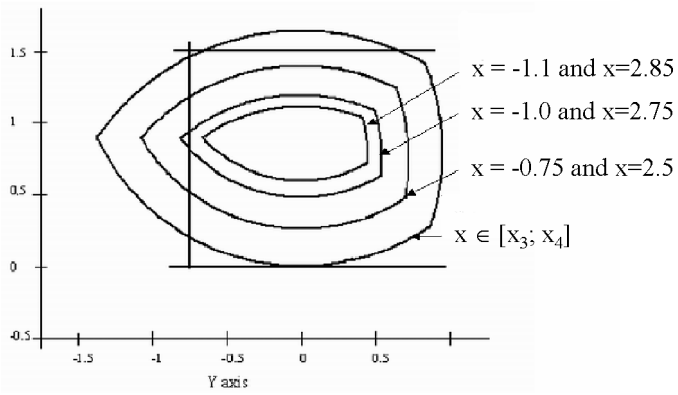

Figure 10: The change of the workspace of the Gantry-Tau robot in the YZ-plane as a function of x.

Fig. 10 shows different workspace areas for 6 different x-coordinates and for the section $[x_3; x_4]$, in which the cross-sectional area is constant. The specific values for the boundaries $x_1, \cdots, x_6$ and the kinematic parameters $L_1, \cdots, L_8$ are listed in Section 5.

4 Optimisation Problem

The workspace volume optimisation is based on the least-squares nonlinear optimisation function *lsqnonlin* in Matlab. The optimisation problem is expressed as

$$\begin{aligned} &\max V(Q_1, Q_2) \quad (36)\\ &\text{subject to}\\ &Q_1 > 0\\ &Q_2 > 0 \end{aligned}$$

V is a nonlinear function containing squares and square-roots of Q_1 and Q_2, seen from equations (16)-(19). Hence, the total workspace volume as a function of the two support frame design parameters Q_1 and Q_2 will be maximised. Alternatively, a cross-sectional workspace area in the YZ plane could be maximised as in [Johannesson, 2004]. The volume is preferred as the cross-sectional area depends on the X position. For the optimisation problem described above, the arm lengths are fixed constants. One or more of these lengths can be made unconstrained and part of the optimisation problem. However, if all the arm lengths are unconstrained and have no upper limits, the workspace volume will go to infinity. In practice, long arm lengths have to be avoided to achieve the required machine stiffness.

5 Results

Two different scenarios were tested. In the first scenario $Q_2 = 2Q_1$, which has been a common design selection in the previous prototypes of the Gantry-Tau. In the second scenario, both Q_1 and Q_2 were unconstrained. The design parameters for the Gantry-Tau were chosen equal to the prototype in Fig. 4 and given as follows.

$$\begin{aligned} &L_1 = L_2 = L_3 = 1.5\\ &L_4 = 0.080 \quad L_5 = 0.155\\ &L_6 = 0.078 \quad L_7 = 0.255\\ &L_8 = 0.112 \quad Y_{\text{offs}} = 0.1 \end{aligned}$$

where all the dimensions are in metres. With these lengths, the boundaries $x_1, \cdots, x_6$ are given below.

$$\begin{aligned} x_1 &= -L_{3d}^{'}\sin(\frac{\pi}{4}) = -1.265\\ x_2 &= X_L = 0\\ x_3 &= x_2 + Y_{offs} = 0.1\\ x_4 &= x_5 - Y_{offs} = 1.65\\ x_5 &= X_U = 1.75\\ x_6 &= L_{3d}^{'}\sin(\frac{\pi}{4}) + 1.75 = 3.02\\ \delta &= 0.03 \end{aligned}$$

The optimal results for Q_1 and Q_2 in the first scenario are:

$$\begin{aligned} Q1 &= 0.7265m\\ Q_2 &= 1.4531m\\ V &= 8.2719m^3 \end{aligned}$$

The optimal results for the unconstrained case are:

$$\begin{aligned} Q_1 &= 0.7805m\\ Q_2 &= 1.4454m\\ V &= 8.2903m^3 \end{aligned}$$

These results confirm that the common design selections for the initial prototypes of the Gantry-Tau are close to optimal. The results for the second case is only slightly larger than the first case. Q_2 should be approximately equal to the arm length when all the arms have equal lengths and Q_1 should be equal to approximately half the arm length.

To show that the proportion $Q_2 = 2Q_1$ is not always optimal, one of the link lengths L_{3d} is changed to 1.0 metre. The new unconstrained optimisation results with the new link length are given below.

$$\begin{aligned} Q_1 &= 0.8442m\\ Q_2 &= 1.0639m\\ V &= 4.9938m^3 \end{aligned}$$

This third result shows that the 2-to-1 ratio between Q_1 and Q_2 is no longer optimal and is an example of a design problem that would be difficult to achieve manually.

Individual arm lengths can be used to increase the workspace by considering Fig. 5. Increasing L_1 will for example make it possible to make use of the area between the circle intersections $[y_{13}; z_{13}]$, $[y_{12}; z_{12}]$ and $[y_{23}; z_{23}]$. If the linear modules $1, 2, 3$ are not mounted with 1 in the middle between 2 and 3 but instead on the line $z = 0$ the border line $y = -Q_1$ will disappear and the common area for the circles of L_2 and L_3 can be used all the way to $[-y_{23}; -z_{23}]$. It should also be noted that there is no collisions between the TCP and the actuators at $z = 0$ for $y > 0$ and at $z = 1.5$ for $y > 0$. Therefore, if there are no other boundaries such as the floor at $z \leq 0$, the workspace could be increased for $y > 0$ if L_2 and L_3 are increased. However, using longer L_2 and L_3 to make use of the space for $y > 0$ makes it necessary to model limitations because of collisions between the links and actuators 2 and 3.

To show that individual arm lengths can be used to increase the workspace additional optimisation was done. In a fourth optimisation case Q_1, Q_2, L_2 and L_3 were unconstrained while L_1 was fixed. The results for this case are given below.

$$\begin{aligned} Q_1 &= 0.9949m \\ Q_2 &= 1.5995m \\ L_2 &= 1.9684m \\ L_3 &= 1.9707m \\ V &= 10.9721m^3 \end{aligned}$$

This shows that the workspace can be increased by more than 32% compared to the first result whereas the design parameters Q_1, Q_2, L_2 and L_3 increased between 10% and 37%.

In a typical design case for the Gantry-Tau, the end application will determine the required workspace. Hence, lower and upper bounds on the cross-sectional area and the volume will be given. In such a case, all the individual arm lengths can be unconstrained.

6 Conclusion

In this paper a new geometric approach for describing the cross-sectional workspace area of the triangular-link version of the Gantry-Tau has been developed. The functional dependency of the cross-sectional workspace area on the robot's x-coordinate is used to calculate the total workspace volume. This workspace volume is maximised by solving a nonlinear least squares optimisation problem. The optimisation yields two design parameters which determine the placement of two of the linear actuators with respect to the third actuator. For the standard design case when all the arms have the same lengths, the optimisation results in a solution which is close to existing designs of the Gantry-Tau that until now have been designed by experience and intuition. The main benefit of the method developed in this paper becomes evident for Gantry-Tau manipulators with different arm lengths.

The future development of the work presented in this paper will be to incorporate manipulator stiffness as an optimisation criterion. This would effectively place an upper bound on the arm lengths. A second extension would be to account for collisions between the links inside the grey area in Fig. 5. A third extension would be to consider multi-body dynamic optimisation, taking the lower bounds on the first resonance frequencies of the machine into account.

References

[Angeles, 1985] J. Angeles. *On the Numerical Solution of the Inverse Kinematics Problem.* Int. J. Robotics Res., Vol. 4, no. 2, pp.21-37, 1985.

[Brogårdh, 2002] T. Brogårdh. *PKM Research - Important Issues,as seen from a Product Development Perspective at ABB Robotics.* In Proc. of the Workshop on Fundamental Issues and Future Research Directions for Parallel Mechanisms and Manipulators. October 3-4, 2002, Quebec, Canada.

[Brogårdh, 2005] T. Brogårdh, S. Hanssen and G. Hovland, *Application-Oriented Development of Parallel Kinematic Manipulators with Large Workspace.* In Proc. of the 2nd International Colloquium of the Collaborative Research Center 562: Robotic Systems for Handling and Assembly, Braunschweig, Germany, May 2005, pp. 153-170.

[Dashy, 2002] A.K. Dashy, S.H. Yeoy, G. Yangz, I.-H.Chery. *Workspace Analysis and Singularity Representation of Three-Legged Parallel Manipulators.* In Proc. of the Seventh International Conference in Control, Automation, Robotics And Vision, Singapore, 2002, pp. 962-967.

[Goldenberg, 1985] A. A. Goldenberg and B. Benhahib and R. G. Fenton. *A Complete Generalized Solution to the Inverse Kinematics of Robots.* ITEE Journal Robotics Automat., Vol. RA-1, no. 1, pp.14-20, 1985.

[Huang, 2004] Tian Huang, Meng Li, Zhanxian Li, Derek G. Chetwynd, David J. Whitehouse. *Optimal Kinematic Design of 2-DOF Parallel Manipulator With Well-Shaped Workspase Bounded by a Specified Conditioning index.* IEEE Transactions on Robotics and Automation, Vol. 20, No. 3, June 2004.

[Johannesson, 2004] S. Johannesson, V. Berbyuk and T. Brogårdh. *A New Three Degrees of Freedom Parallel*

Manipulator. In Proc. of the 4th Chemnitz Parallel Kinematics Seminar, Germany, April 20-21 2004, pp. 731-734.

[Lee, 1999] Min Ki Lee, Kun Woo Park. *Kinematic and Dynamic Analysis of A Double Parallel Manipulator for Enlarging, Workspace and Avoiding Singularities*. IEEE Transactions on Robotics and Automation, Vol. 15, No. 6, December 1999.

[Merlet, 1995] J.-P. Merlet. *Designing a Parallel Manipulator for a Specific Workspace*. Institut National de Recherche en Informatique et en Automatique, Tech. Rep 2527, April 1995.

[Yun, 2004] Yuan Yun, Liping Wang, Liwen Guan. *Dimensional Synthesis of a 3-DOF Parallel Manipulator*. IEEE International Conference on Systems, Man and Cybernetics, 2004, pp. 5317-5323.